Catecholaminergic neurons in medullary nuclei are among the post-synaptic targets of descending projections from infralimbic area 25 of the rat medial prefrontal cortex

Neuroscience 144 (2007) 623–635

CATECHOLAMINERGIC NEURONS IN MEDULLARY NUCLEI ARE AMONG THE POST-SYNAPTIC TARGETS OF DESCENDING PROJECTIONS FROM INFRALIMBIC AREA 25 OF THE RAT MEDIAL PREFRONTAL CORTEX

P. L. A. GABBOTT,[a,b]* T. WARNER[a] AND S. J. BUSBY[b]

[a]*Department of Biological Sciences, The Open University, Milton Keynes, MK7 6AA UK*

[b]*University Department of Pharmacology, Mansfield Road, Oxford, OX1 3QT UK*

Abstract—The infralimbic (IL) 'visceromotor' area of the rat medial prefrontal cortex projects to strategic subcortical nuclei involved in autonomic functions. Central among these targets are the nucleus tractus solitarius (NTS) and the rostral ventrolateral medulla (rVLM). By combining tract-tracing using the anterograde tracer biotinylated dextran amine (BDA) with immunolabeling for tyrosine hydroxylase (TH; an enzyme marker of catecholaminergic neurons), a limited proportion of BDA-labeled IL axonal boutons in the NTS and rVLM was found to be closely associated with TH immunopositive (+) target structures. Such structural appositions were mainly located proximally over the labeled dendritic arbors of identified TH+ neurons.

Quantitative ultrastructural examination revealed that in NTS, TH+ dendritic shafts comprised 7.0% of the overall post-synaptic target population innervated by BDA-labeled IL boutons, whereas TH+ dendritic spines represented 1.25% of targets. In rVLM, TH+ shafts represented 9.0% and TH+ spines 2.5% of IL targets. Labeled IL boutons established exclusively asymmetric Gray Type 1 (presumed excitatory) synaptic junctions.

The results indicate that subpopulations of catecholaminergic neurons in the NTS and rVLM are among the spectrum of post-synaptic neurons monosynaptically innervated by descending 'excitatory' input from IL cortex. Such connectivity, albeit restricted, identifies the potential direct influence of IL cortex on the processing and distribution of cardiovascular, respiratory and related autonomic information by catecholaminergic neurons in the NTS and VLM of the rat.

*Correspondence to: P. L. A. Gabbott, Department of Biological Sciences, The Open University, Milton Keynes, MK7 6AA UK. Tel: +44-1908-659469; fax: +44-1908-654167.
E-mail address: p.l.gabbott@open.ac.uk (P. L. A. Gabbott).

Abbreviations: ACd, dorsal anterior cingulate cortex (area 24b); B, Bregma; BDA, biotinylated dextran amine; BLA, basolateral nucleus of the amygdala; CEA, central nucleus of the amygdala; DAB, 3,3′-diaminobenzidine; DMH, dorsomedial hypothalamic nucleus; DMX, dorsal motor nucleus of the vagus; IL, infralimbic cortex (area 25); LH, lateral hypothalamus; MAP, mean arterial blood pressure; mPFC, medial prefrontal cortex; NA, noradrenergic; NTS, nucleus tractus solitarius; P, peduncular cortex; PB, phosphate buffer; PBN, parabrachial nucleus; PL, prelimbic cortex (area 32); PVN, paraventricular hypothalamic nucleus; rVLM, rostral ventrolateral medulla; SG, slate gray; TH, tyrosine hydroxylase; TH+, tyrosine hydroxylase immunopositive; VLM, ventrolateral medulla; vlPAG, ventrolateral periaqueductal gray; vmPFC, ventromedial prefrontal cortex; VS, ventral striatum.

Key words: visceromotor cortex, NTS, rVLM, cardiovascular functions, autonomic functions.

The medial prefrontal cortex (mPFC) is directly involved in the integration of cognitive and autonomic functions underlying flexible goal-directed behavior (Cechetto and Saper, 1990; Neafsey et al., 1993; Loewy, 1991; Owens et al., 1999; Van Eden and Buijs, 2000; Drevets, 2000; Uylings et al., 2000; Heidbreder and Groenewegen, 2003). In the rat, the mPFC is composed of the anterior cingulate (ACd, Brodmann area 24b), prelimbic (PL, area 32), infralimbic (IL, area 25), and peduncular (P) cortices (Neafsey et al., 1993; Gabbott et al., 2005; Resstel and Corrêa, 2006b).

Anatomical and physiological evidence indicates that areas of dorsal (d) mPFC (ACd and dPL cortices) process cognitive information, whereas regions of ventromedial prefrontal cortex (vmPFC) (vPL, IL and P cortices) are also involved in autonomic and visceral functions, especially, cardiovascular and respiratory activities (Hardy and Mack, 1990; Neafsey, 1990; Loewy, 1991; Neafsey et al., 1993; Spyer, 1994; Fisk and Wyss, 2000; Uylings et al., 2003; Heidbreder and Groenewegen, 2003). Descending efferent projections from vmPFC, in particular IL cortex, innervate a wide range of subcortical autonomic centers, including the nucleus tractus solitarius (NTS) and ventrolateral medulla (VLM), brain stem nuclei strategically involved in cardiopulmonary activities (Agarwal and Calarescu, 1992; Van Giersbergen et al., 1992; Dampney, 1994; Owens and Verberne, 1996, 2000, 2001; Owens et al., 1999). Indeed, stimulation of the vPL and IL cortices is known to influence arterial blood pressure and blood flow through specific vascular beds (Owens and Verberne, 2001). As a result, the vmPFC has been considered to represent a 'visceromotor' territory of the rodent PFC (Terreberry and Neafsey, 1987; Ruit and Neafsey, 1990; Loewy, 1991; Neafsey et al., 1993; Resstel and Corrêa, 2006a,b).

Although the pathways from IL cortex to autonomic centers in the brain stem have been described in previous light microscope studies (Sesack et al., 1989; Hurley et al., 1991; Takagishi and Chiba, 1991; Van Eden and Buijs, 2000; Heidbreder and Groenewegen, 2003; Vertes, 2004; Gabbott et al., 2005), the ultrastructural identities and neurochemical content of the post-synaptic target neurons have not been investigated in detail (Zagon et al., 1994; Torrealba and Müller, 1999). Of specific functional significance is that catecholaminergic neurons in the NTS and rostral ventrolateral medulla (rVLM) are strategically in-

0306-4522/07$30.00+0.00 © 2006 IBRO. Published by Elsevier Ltd. All rights reserved.
doi:10.1016/j.neuroscience.2006.09.048

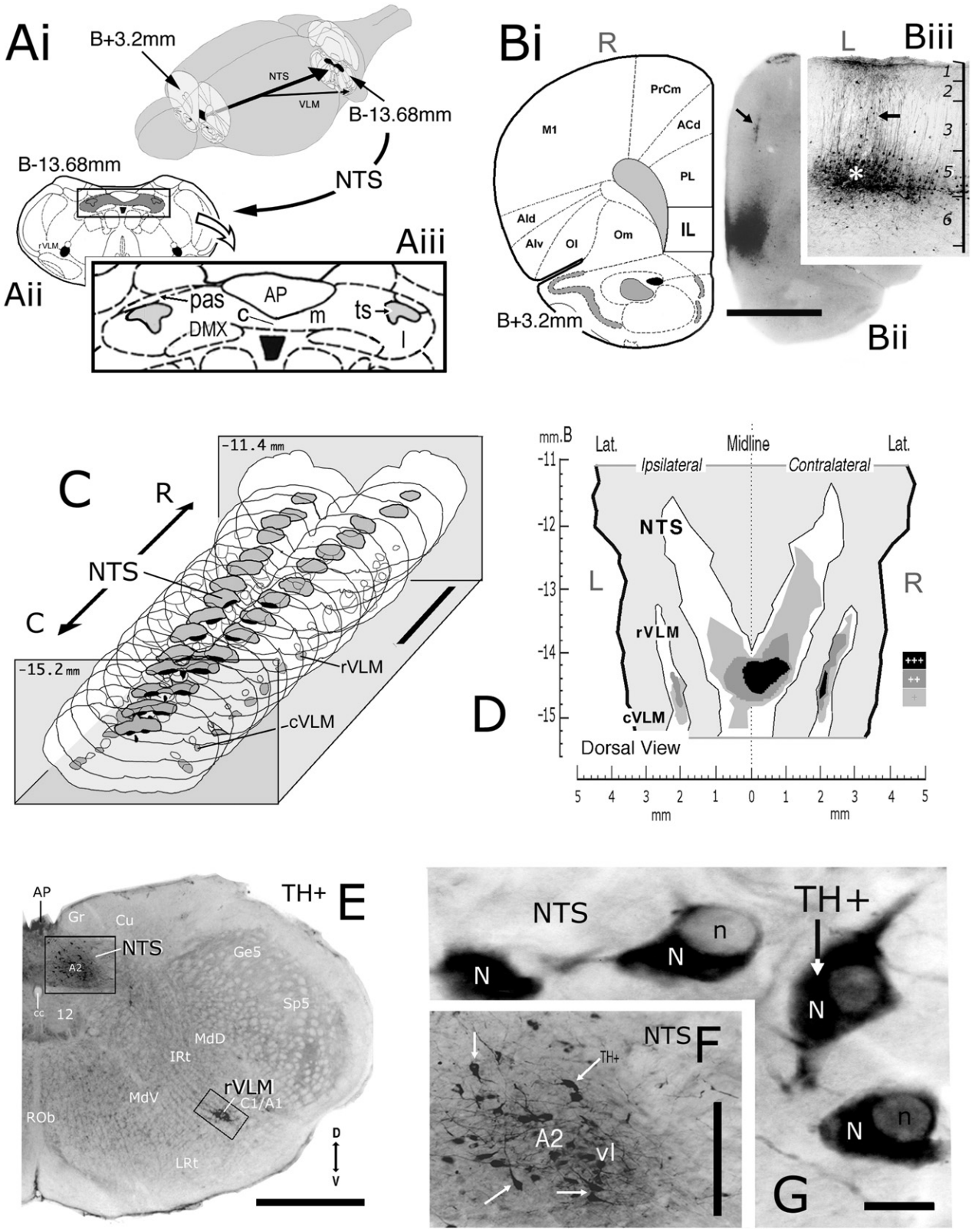

Fig. 1. (Ai) Schematic diagram of rat brain showing the descending projection from IL cortex (black region, located at +3.2 mm in front of B) to the NTS and the rVLM (located at −13.68 mm behind B). In Aii, the positions of the NTS (gray) and rVLM (black) are shown. The NTS is shown enlarged in Aiii. Note that some IL projection neurons have divergent axons (asterisk) innervating both NTS and VLM (Gabbott et al., 2005). (Bi) Drawing of section from +3.2 mm anterior to B. (Bii) Histological section (same level as Bi) showing the umbra of the BDA injection site (dark DAB-labeled region)

volved in the central control of cardiovascular, respiratory and other autonomic functions in the rat (Kubo et al., 1990; Yasui et al., 1991; Dampney, 1994; Murphy et al., 1994; Owens and Verberne, 1996, 2000, 2001; Owens et al., 1999; Dampney et al., 2003; Krout et al., 2005; Resstel and Corrêa, 2006a,b). The principal aim of this study was to use tract-tracing methods in combination with immunocytochemical and light/electron microscopical techniques to ascertain whether catecholamine-containing neurons in the NTS and rVLM were post-synaptic targets of descending input from IL cortex.

Such anatomical evidence would provide novel and significant information further defining brain stem neural circuitry whereby layer 5 projection neurons in the 'visceromotor' subregion of vmPFC have the potential to directly modulate central cardiovascular and related functions in the rat (Neafsey et al., 1993; Uylings et al., 2000, 2003; Groenewegen and Uylings, 2000; Van Eden and Buijs, 2000; Heidbreder and Groenewegen 2003; Vertes, 2004; Krout et al., 2005). Part of this investigation has been reported previously in abstract form (Bacon and Gabbott, 1997).

EXPERIMENTAL METHODS

Twenty adult male Sprague–Dawley rats (230–280 g) were used in the present study. The rats were maintained on a 12-h light/dark cycle, with *ad libitum* access to food and water.

The animals were anesthetized with equithesin (0.3 ml/100 g body weight i.p.; Millenbruck and Wallinga, 1946) and iontophoretic injections [pulsed (0.1–1.0 Hz) DC current (2–10 μamp) for 15–20 min] of the anterograde pathway tracer biotinylated dextran amine [BDA; 10,000 MWt, Molecular Probes, Invitrogen Ltd., Paisley, Glasgow, UK; 5–10% in 0.01 M phosphate buffer (PB), pH 7.4] were made into sites located in the left hemisphere within the following coordinate ranges relative to Bregma (B): anterior/posterior +2.5 mm to +3.2 mm; mediolateral 0.75 mm to 0.85 mm; and dorsoventral −4.8 mm to −5.4 mm (Fig. 1A, B, C; Swanson, 1998). These coordinates lie within the IL area of the mPFC (Swanson, 1998; Gabbott et al., 2005).

After a survival period of 7–10 days the animals were reanaesthetized and transcardially perfused, initially with 50 ml physiological saline (0.9% NaCl), followed by a 400–500 ml fixative solution containing 0.1–1.0% glutaraldehyde and 2–4% paraformaldehyde in 0.1 M PB (pH 7.4) (Bolam, 1992). All surgical and animal procedures were performed in strict accordance with the Society for Neuroscience 'Policy on the use of animals in neuroscience research' and were licensed under the UK Animals (Scientific Procedures) Act, 1986. No post-operative complications were observed in animals. The experimental design minimized the number of animals used and kept any suffering to a minimum.

Following perfusion, the brains were carefully removed and serial coronal Vibratome sections (50–100 μm thick) cut through the injection site in vmPFC and throughout the rostrocaudal extent of the brain stem (Fig. 1C). To visualize the IL cortical injection site and the anterogradely labeled terminal arbors of IL axonal afferents to brain stem nuclei (Fig. 1B, C), selected sections from both regions were processed using an ABC Vectastain kit (Vector Laboratories, Peterborough, UK) with the chromagen 3,3′-diaminobenzidine (DAB). DAB produces a brown reaction end-product (Bolam 1992). Selected sections were Nissl-counterstained to reveal the areal and laminar organization of the mPFC (Fig. 1Bi) and the cytoarchitecture of the brainstem (Fig. 1C, D; Paxinos et al., 1999; Gabbott et al., 2005).

Anterograde tract-tracing combined with tyrosine hydroxylase (TH) immunocytochemistry

Tissue sections, with extensive BDA-labeled IL axonal afferents in the NTS and rVLM (Bacon and Gabbott, 1997), were further processed immunocytochemically to localize TH, the key rate limiting enzyme in the biosynthesis of catecholamines. TH is a recognized cell marker for catecholamine containing neurons in the NTS and rVLM (Halliday and McLachlan, 1991; Dampney and Horiuchi, 2003).

Tissue sections were incubated with a monoclonal anti-TH antibody (mouse anti-TH, diluted 1:1000–5000 in phosphate-buffered saline, T2928 Sigma-Aldrich, Poole, UK) for 48 h at 4 °C, then in biotinylated horse anti-mouse antibody (1:200, Vector Laboratories), and finally in avidin–biotin peroxidase complex (ABC, Vector Laboratories) for 2 h at room temperature. TH immunolabeling was visualized using the slate gray (SG) peroxidase staining kit (Vector Laboratories, Nottingham, UK) which produces a distinct gray/gray–black label (Hussain et al., 1996; Gabbott et al., 2002). Specific immunolabeling was absent in control incubations where the primary antibody and/or secondary link antibody had been omitted.

Tissue sections for light-microscopy were air-dried, dehydrated using conventional methods and finally embedded on glass slides in DPX (Bolam, 1992). Sections for combined light/electron-microscopical examination, were treated with osmium tetroxide [1% OsO_4 (aq), 40 min], dehydrated in an ascending alcohol series (with 1% uranyl acetate in the 70% alcohol), passed swiftly through fresh propylene oxide, flat-embedded between a glass slide and a coverslip in Durcupan resin (ACM Fluka) then cured at 60 °C for 48 h (Bolam, 1992). Sections were extensively examined in a light microscope and interesting structures recorded by line-drawings, photomicrographs or digital images.

In two complete sets of serial sections, the mediolateral density distribution of the BDA labeled IL fibers in NTS and VLM were assessed in each section. The densities of the labeled fibers were graded as light (+), moderate (++) and heavy (+++). Projection maps were subsequently constructed of the mediolateral/rostro-

located centrally in IL cortex. Micropipette track (black arrow). Scale bar=2.5 mm. (Biii) Penumbra of the BDA injection site (white asterisk) centered on deep layer 5. Radially oriented BDA-labeled fibers (presumed apical dendrites of labeled layer 5 pyramidal cells) ascend through the cortex (black arrow) and ramify in layer 1. (C) Drawings of serial sections (spaced approx. 250 μm apart) from −11.4 mm to −15.2 mm behind B showing the rostrocaudal extent of the NTS and the rostral (r) and caudal (c) sectors of the VLM. Note the bilateral distribution of both nuclei, particularly the rostral to caudal 'Y-like' shape of the NTS (see also dorsal view in D). DMX is indicated (black area). Scale bar=1 mm. (D) Diagrammatic dorsal view of the rat midbrain [*y* axis is distance posterior to B (mm); *x* axis is distance lateral to midline (mm); R right, L left]. The rostrocaudal and mediolateral boundaries of the NTS and r/c VLM are shown. The 'relative density distribution' of identified axonal swellings anterogradely labeled following injections of BDA into the IL within both nuclei is shown. The relative grading in the densities of BDA-labeled axonal fibers in the NTS and VLM is given as light (+), moderate (++) and heavy (+++). Note high density of labeled infralimbic axonal fibers in the c and rVLM and the more extensive projection to the contralateral anterior/rostral sectors of both nuclei. (E) Light micrograph of rat brain stem section showing TH immunolabeling of the C1/A1 and A2 catecholaminergic cell groups (regions of dark staining) in the VLM and NTS (respectively). The boxed region in the NTS shown enlarged in F. Scale bar=1 mm. (F) Enlargement of area outlined in E showing TH+ immunoreactive neurons (white arrows) defining the catecholaminergic A2 cell group in the lateral part of the NTS. Scale bar=250 μm. (G) Characteristic light microscopical appearance of TH+ neurons (N) in the A2 cell group of the lateral NTS. Cell nuclei (n) are unlabeled. Scale bar=10 μm.

caudal distribution of the labeled axonal fibers as viewed from the dorsal surface (Fig. 1C, D).

Ultrastructural investigations

The electron microscopical features of identified labeled objects (either anterogradely labeled BDA axonal varicosities and/or TH-immunolabeled elements) seen in the light microscope were studied ultrastructurally using a correlated light and electron microscopical examination procedure described previously in detail (Bolam, 1992). In brief, serial ultrathin sections (70 nm thick) were cut through the same identified neural elements seen in the light microscope, collected on Formvar-coated single slot grids, stained with Reynold's lead citrate and examined ultrastructurally.

In the electron microscope, anterogradely labeled IL axonal fibers and varicosities that were revealed using DAB possessed the characteristic dark precipitate end-product of the peroxidase reaction (Bolam, 1992). In comparison, TH-immunoreactive structures labeled using Vector SG contained a distinctive granular reaction end-product embedded in a fine diffuse background label (Hussain et al., 1996; Gabbott et al., 2002). Structures labeled with DAB or SG could be readily distinguished in the electron microscope (see Fig. 4E, F, G), especially using the correlated light/electron microscope procedure adopted here (Hussain et al., 1996). Electron micrographs of identified structures were produced photographically, scanned digitally and electronic image files created.

A quantitative analysis was undertaken of the cellular targets innervated by the anterogradely labeled IL boutons in contralateral NTS and rVLM. A 'systematic random non-serial' sampling procedure was used to quantify the percentage distribution of post-synaptic structures (e.g. spines heads, dendritic shafts, somata and axon initial segments) innervated by labeled presynaptic IL boutons (Bacon et al., 1996). A combined sample of 600 labeled presynaptic IL boutons in the ventrolateral NTS and rVLM in two animals was analyzed (200 boutons in NTS/100 boutons in rVLM per animal: Howard and Reed, 2005). Only labeled boutons displaying distinct pre- and post-synaptic membranes and well-defined target structures were included in the analysis. To avoid the repeated sampling of individual synaptic boutons (max. diam: 1.5 μm), quantitative estimates were made in ultrathin sections spaced more than about 1.75 μm apart (i.e. approximately every 25th ultrathin section). In the same non-serial sections, an assessment was also made of the percentage (P% in the equation below) that asymmetrical synapses formed by IL boutons (IL.asym) composed of the total population of asymmetric synapses present (T.asym). Perforated or complex asymmetric synaptic junctions associated with a single post-synaptic element were considered to represent a single synaptic junction. An estimate of P% (=[IL.asym/T.asym]×100) was obtained for both NTS and rVLM. The mean profile areas of 50 randomly selected labeled presynaptic IL boutons taken from both medullary structures were calculated using NIH image measuring program (http://rsb.info.nih.gov/nih-image).

Digital images were finally imported into Adobe Photoshop® CS2 where photographic montages were composed, adjusted for gray levels, contrast and brightness, and illustrative figures prepared.

RESULTS

Injections of BDA into IL cortex

Iontophoretic injections of the anterograde tracer BDA into IL cortex were centered on lower layer 5 and occupied a large proportion of the target area (Fig. 1Bi, Bii, Biii). Injection sites in IL cortex were located between AP coordinates B +2.4 mm and B +3.3 mm (Fig. 1B; Swanson, 1998).

Following suitable histological processing, the central umbra of the injection sites displayed numerous darkly labeled cells in layers 3, 5 and 6 of IL cortex (Fig. 1Bii). In the injection penumbra, the majority of labeled somata were present in layer 5. Such cells were clearly pyramidal in morphology and frequently possessed a single prominent radially oriented BDA labeled process (presumed apical dendrite) that ascended perpendicular to the pial surface through the superficial layers to terminate in layer 1 (Fig. 1Biii). The precise areal and laminar position of injection sites was confirmed in adjacent Nissl-stained sections (Gabbott et al., 2005).

Light microscopical observations

Following injections of BDA into IL cortex, anterogradely labeled fibers were found in specific cortical and subcortical target structures as described previously (Sesack et al., 1989; Hurley et al., 1991; see also Fig. 3 in Van Eden and Buijs, 2000). Labeled IL fibers were found in the following brainstem structures: ventrolateral periaqueductal gray (vlPAG), parabrachial nucleus (PBN), Barrington's nucleus, NTS, VLM as well as the nucleus ambiguus and the dorsal motor nucleus of the vagus (DMX).

Abbreviations used in the figures

AId	dorsal agranular insular cortex
AIv	ventral agranular insular cortex
AP	area postrema
c	commissural part of nucleus tractus solitarius
C	caudal
cc	central canal
Cu	cuneate nucleus
cVLM	caudal ventrolateral medulla
D	dorsal
DP	dorsal peduncular cortex
Ge5	gelatinous layer of the caudal spinal trigeminal nucleus
ft	fiber tract
Gr	gracile nucleus
IRt	intermediate reticular nucleus
l	lateral nucleus tractus solitarius
LRt	lateral reticular tract
M	medial nucleus tractus solitarius
M1	primary motor cortex
MdD/V	medullary reticular nucleus pars dorsalis/ventralis
Ol	lateral orbital cortex
Om	medial orbital cortex
orbital lat	lateral orbital cortex
orbital med	medial orbital cortex
pa	parasolitary nucleus
PrCm	medial precentral cortex
R	rostral
ROb	nucleus raphe obscurus
Sp5	spinal trigeminal tract
ts	tractus solitarius
V	ventral
12	hypoglossal nucleus

Labeled IL fibers in NTS and VLM

All BDA injections in IL cortex produced bilateral anterograde labeling of fine caliber varicose axonal arbors in both the NTS and rVLM (see Fig. 4A). However labeled varicose fibers were denser and more widely distributed in the contralateral target structures with the number of labeled axonal varicosities being much greater in NTS than in rVLM (Fig. 1D).

In contralateral NTS, anterogradely labeled IL fibers were present rostrally but were more numerous toward the intermediate and caudal sectors (Fig. 1D). A similar rostrocaudal distribution pattern was present in rVLM (Fig. 1D). Labeled varicose fibers were particularly concentrated in caudal NTS where they ramified extensively throughout the commissural, mediolateral, intermediate, ventral, interstitial, dorsolateral, and lateral subdivisions, but were most dense in the ventrolateral aspects (Van Giersbergen et al., 1992). Injections into more posterior regions of IL cortex (c. B +2.5 mm) produced a comparatively greater number of anterogradely labeled IL fibers in middle and caudal NTS, as well as rVLM, compared with injections located more rostrally. Of note is that anterogradely labeled IL fibers were also present in the intermediate and caudal (c) sectors of the VLM, however the number was reduced compared with the innervation of the rVLM. Anterogradely labeled IL axonal swellings in both the NTS and VLM were variable in size (range 0.2–1.54 μm in diameter; Figs. 2A, B; 4E) with a prevalence of small-sized varicosities.

Following BDA injections into IL cortex anterograde labeling in the NTS and VLM only consisted of varicose axonal fibers; dendritic and somatic labeling was absent. This excludes the possibility that BDA was transported retrogradely; an unlikely occurrence since direct ascending pathways from these brainstem nuclei to the mPFC have not been demonstrated. Consequently it is considered that the identified varicose plexuses in the NTS and VLM were the anterogradely labeled terminal arbors of descending axonal fibers from injection sites in IL cortex.

Tyrosine hydroxylase immunopositive (TH+) neurons in NTS and rVLM

Of note is that TH+ immunoreactive structures were present throughout most of the depth of the histological sections, indicating good penetration of the antisera into the interior of the tissue.

Populations of TH+ neurons were present along the rostrocaudal axis of the NTS and VLM as described previously (Fig. 1E, F; see also Van Giersbergen et al., 1992; Dampney, 1994). The characteristic somatodendritic and axonal morphologies as well as distributions of TH+ neurons in the NTS have been reported in detail elsewhere (Halliday and McLachlan, 1991; Jia et al., 1997). In brief, TH+ immunoreactivity was present in neuronal cell bodies, smooth and spiny dendrites, as well as fine fragmented varicose fibers that were morphologically distinct from brown DAB labeled afferent IL fibers (Fig. 1G; 2Ai–iii, Bi, ii; 3A, C; 4A, E). TH+ neurons displayed various somatodendritic morphologies and orientations ranging from bitufted cells with oval somata oriented perpendicularly along the mediolateral axis of the NTS, to large multitufted cells with long radiate dendrites and ovoid cell bodies (Fig. 3A, C; 4E). In rVLM, TH+ neurons were tufted cells with long dendritic processes of varying thicknesses aligned along the fiber tracts traversing through this structure. Nuclei of TH+ neurons were devoid of immunolabel (Figs. 1G; 3A; 4E).

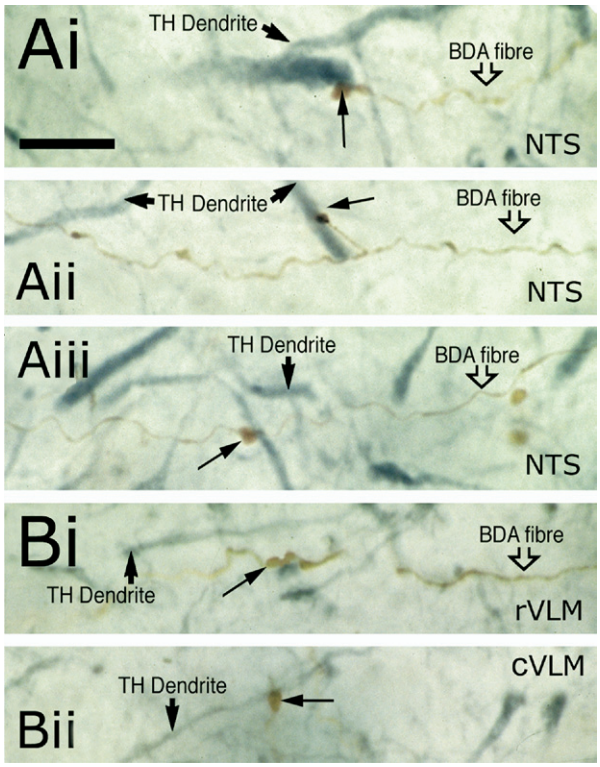

Fig. 2. (Ai–iii) Examples of brown (DAB visualized) BDA containing fibers from IL cortex coursing in the caudolateral subdivisions of the NTS. These fibers ramify near gray (SG visualized) TH+ dendrites. Several brown BDA IL axonal swellings are in close apposition (long thin arrows) with gray TH+ dendritic shafts. Scale bar=10 μm in Ai. (Bi, ii) Examples of brown (DAB visualized) BDA containing fibers from the IL cortex traversing the rVLM (Bi) and cVLM (Bii). Brown BDA IL axonal swellings closely abut (long thin arrows) gray TH+ dendritic shafts. For interpretation of the references to color in this figure legend, the reader is referred to the Web version of this article.

Immunopositive dendritic spines could be found over the more distal processes of TH+ neurons in both NTS and rVLM (Fig. 3C, cells 7, 8, 11). However in many cases spine necks were frequently too thin, or too weakly immunolabeled to be seen with clarity.

Relationship of labeled IL axonal varicosities with TH+ profiles

Careful observation revealed brown DAB-labeled IL axonal swellings closely apposed to gray SG immunolabeled dendritic shafts of identified TH+ neurons in NTS and (Fig. 2Ai–iii, Bi, ii). Although such appositions were not numerous, they could be found throughout rostral NTS and VLM, and with increasing frequencies in caudolateral NTS and

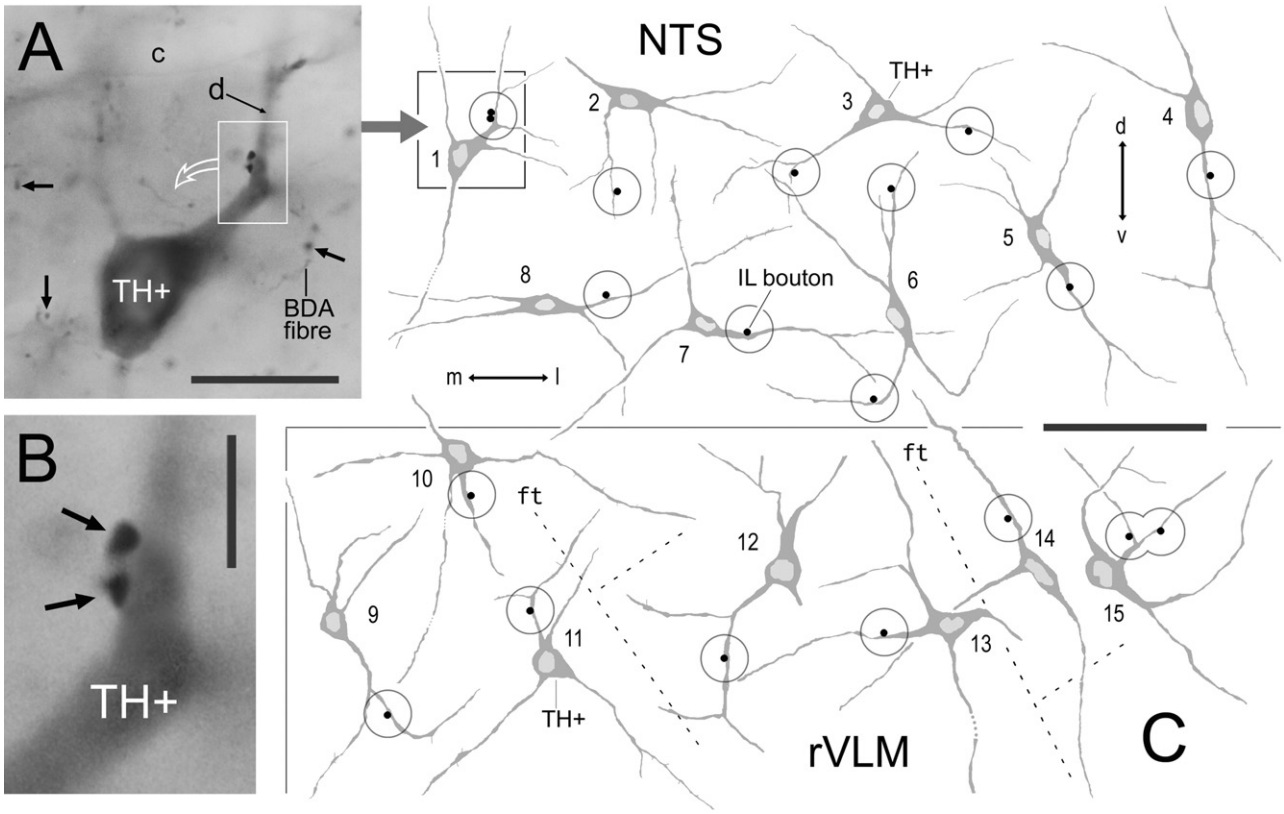

Fig. 3. (A) Light micrograph of a TH+ neuron and labeled dendrite (d) in lateral NTS. A BDA-labeled axonal fiber from IL cortex courses in the vicinity of the dendritic arbor. (TH immunoreactivity visualized with SG and BDA containing structures revealed using DAB; see Fig. 2). Identified axonal swellings along IL fibers are indicated (black arrows). Two dark DAB-labeled IL axonal varicosities abut the second order dendritic segment (d) of the labeled TH+ neuron (boxed region). Capillary, c. Scale bar=20 μm. (B) Enlargement of the boxed region shown in A showing the two IL axonal varicosities (arrows) in close structural contact with the TH+-immunolabeled dendritic shaft. Scale bar=5 μm. (C) Line drawings of TH+ neurons in NTS (cells 1–8) and rVLM (cells 9–15) showing the positions of labeled IL axonal varicosities (dark circles) in close contact with the immunolabeled dendritic shafts (encircled). Note that the relative positions of somata have been altered for clarity and that dendritic processes ramify entirely within their respective nuclei. Courses of major ft in rVLM are indicated (dashed lines). Scale bar=100 μm.

toward the posterior region of rVLM and in cVLM (Fig. 2Ai–iii, Bi, ii). In both NTS and rVLM, DAB-labeled varicosities were most commonly found abutting the proximal (primary or secondary) dendritic shafts of identified TH+ neurons (Fig. 3A, B).

In the light microscope, a combined survey of 352 TH+ neurons from NTS and VLM (with well-labeled dendritic arbors) revealed that 41 of these cells had brown DAB-labeled IL boutons abutting their immunolabeled processes (Fig. 3A, B, C). A maximum of two labeled IL axonal varicosities was found to be associated with an individual TH+ neuron (Figs. 3C, cells 1, 6 and 15; 4E). On occasion labeled axonal varicosities were apposed to small punctate TH+ structures surrounding immunoreactive distal dendrites, such structures were considered to represent immunolabeled dendritic spine heads emerging from parent dendrites (not illustrated).

Ultrastructural observations

Anterogradely labeled synaptic boutons in NTS and rVLM. In both medullary target regions, anterogradely labeled synaptic boutons from IL cortex were small to medium in size (cross-sectional area of 0.51 $\mu m^2 \pm$ 0.04 μm^2; mean$\pm$S.E.M., n=50; c.f. Torrealba and Müller, 1999). Labeled synaptic boutons could be seen to contain numerous spherical synaptic vesicles and mitochondrial profiles (Fig. 4Ai, ii, B, C). These labeled boutons established exclusively asymmetrical (Gray Type 1; Gray, 1959) synaptic junctions with post-synaptic target structures (Fig. 4Ai, ii; Bi, C).

Dendritic spines and medium/large caliber dendritic shafts (1.2–2.3 μm in mean cross-sectional diameter) were the only post-synaptic targets innervated by labeled IL boutons in both NTS and rVLM (Fig. 4Ai, ii, B, C; Table 1). The somata and axon initial segments of NTS and rVLM neurons did not receive input from labeled IL boutons.

An analysis of a large population of BDA labeled IL boutons from two animals indicated that dendritic spines represented approximately 26% and dendritic shafts 74% of the post-synaptic targets in NTS (Table 1). In contrast, a similar analysis indicated that dendritic spines constituted about 21% and dendritic shafts 79% of the post-synaptic structures in rVLM (Table 1). In non-serial ultrathin sections, the vast majority (>96%) of individual BDA labeled IL synaptic boutons in both NTS

and rVLM were found to innervate a single post-synaptic target structure (Fig. 4Ai, ii, B, C).

A preliminary analysis indicated that the asymmetric synapses derived from IL boutons constituted 5.4% of all asymmetric synaptic junctions in caudal NTS. In rVLM, asymmetric IL synapses represented 3.2% of the overall number of asymmetric synaptic junctions.

Anterogradely labeled IL synaptic input to identified TH+-labeled processes. Table 1 details the percentages that TH+ dendritic shafts and spines composed of the overall target populations innervated by labeled IL synaptic boutons in NTS and rVLM (Fig. 4D, F, G).

Correlated light- and electron-microscopy of labeled IL input to identified TH+ neurons. A total of 21 identified TH+ neurons (14 in caudolateral NTS and seven in rVLM) with anterogradely labeled IL varicosities closely apposed to their immunopositive dendritic processes were selected for ultrastructural investigation using correlated light- and electron-microscopy (Fig. 4E).

Twelve TH+ neurons in NTS were found to receive asymmetric synaptic input from BDA-labeled IL boutons, examples are shown in Figs. 3 and 4E. These axonal boutons were located proximally over the primary and secondary order dendritic shafts of the TH+ cells. In the electron microscope, a maximum number of two labeled synaptic boutons were found to innervate a single identified TH+ neuron in the NTS (Fig. 3E–Gi). Labeled IL synaptic inputs to six of the seven identified TH+ rVLM neurons were confirmed ultrastructurally. In rVLM, IL innervation of TH+ neurons was also located on primary and secondary order dendritic shafts (Fig. 3, cells 9–15) and one TH+ neuron was found to receive labeled synaptic input from two identified IL boutons (Fig. 3, cell 15).

DISCUSSION

Direct projections from the IL cortex to the NTS and VLM in the rodent have been well described in previous retrograde and anterograde tract-tracing light microscope studies (Neafsey et al., 1986; Sesack et al., 1989; Hurley et al., 1991; Takagishi and Chiba, 1991; Van Eden and Buijs, 2000; Cobos et al., 2003; Torrealba and Müller, 1999; Vertes, 2004; Gabbott et al., 2005). However, the neurochemical and ultrastructural identities of the post-synaptic targets, and their relative frequencies, have not been defined.

The main findings of this study are that the dendritic shafts and spines of TH+ neurons in the NTS and rVLM of the rat constitute a modest proportion (<10%) of the post-synaptic targets monosynaptically innervated by descending projections from IL cortex and that labeled IL boutons established asymmetric (Gray Type 1), presumed excitatory, synaptic junctions with target structures. Furthermore, the quantitative data indicated that the TH+ neurons innervated by labeled IL boutons were limited subsets of the overall TH+ neuron populations in these medullary nuclei. The importance of these observations are that they provide novel quantitative ultrastructural evidence for the direct synaptic connectivity of labeled IL boutons and TH+ neurons in the NTS and rVLM.

Methodological considerations

The comparatively low number of close structural associations between anterogradely labeled IL axonal varicosities and TH+ structures in NTS and VLM reported here is unlikely related to methodology. Large BDA injection sites in IL cortex combined with good penetration of antisera into tissue sections will have optimized the potential to observe labeled IL varicosities abutting TH+ somata and dendrites.

Pathways from IL 'visceromotor' cortex to NTS and VLM

In accord with previous tract-tracing studies, anterogradely labeled IL fibers were distributed throughout the rostrocaudal extent of the NTS with an overall contralateral dominance and with the densest labeling at levels caudal to obex (Fig. 1D: Terreberry and Neafsey, 1987; Zagon et al., 1994; Torrealba and Müller, 1999; Van Eden and Buijs, 2000; Cobos et al., 2003; Vertes, 2004). Similarly, tracer injections into posterior IL cortex produced a comparatively dense innervation of VLM (Van Eden and Buijs, 2000; Cobos et al., 2003; Vertes, 2004).

Activity within IL cortex is known to significantly influence cardiovascular functions (Cechetto and Saper, 1990; Hardy and Mack, 1990; Neafsey, 1990; Loewy, 1991; Neafsey et al., 1993; Verberne and Owens, 1998; Fisk and Wyss, 2000; Heidbreder and Groenewegen, 2003; Resstel and Corrêa, 2006a,b). In *anesthetized* animals, electrical stimulation of vmPFC elicits a decrease in mean arterial blood pressure (MAP) coupled with increases in splanchnic and iliac vascular conductance (Verberne et al., 1997; Owens and Verberne, 2000). Sympathoinhibitory mechanisms within the medulla are considered to mediate this depressor response (Hardy and Mack, 1990; Owens et al., 1999; Owens and Verberne, 2000). Furthermore, discrete chemical stimulation of IL cortex in anesthetized rats also produces a significant depressor effect in the femoral artery (circa −16 mm Hg, a reduction of 18%; Busby and Gabbott, unpublished observations). In contrast however, electrical stimulation of the vmPFC in *unanaesthetized* rats produces a sympathetic-related increase in MAP (Tavares et al., 2004) while chemical stimulation with L-glutamate causes a pressor effect with an associated tachycardic response involving activation of sympathetic brainstem circuits (Dampney and Horiuchi, 2003; Resstel and Corrêa, 2006b).

IL cortex not only projects to NTS and VLM but also provides substantial input to other subcortical structures involved in autonomic visceromotor functions that include the lateral, dorsomedial and paraventricular hypothalamic nuclei (LH, DMH, PVN respectively), vlPAG, basolateral and central nuclei of the amygdala (BLA, CEA respectively), locus coeruleus and PBN (Sesack et al., 1989; Hurley et al., 1991; Van Eden and Buijs, 2000; Cobos et al., 2003; Torrealba and Müller, 1999; Fisk and Wyss, 2000; Vertes, 2004). The vmPFC also projects strongly to the core and shell of the ventral striatum (VS) (Ding et al., 2001), a forebrain structure prominently involved in affec-

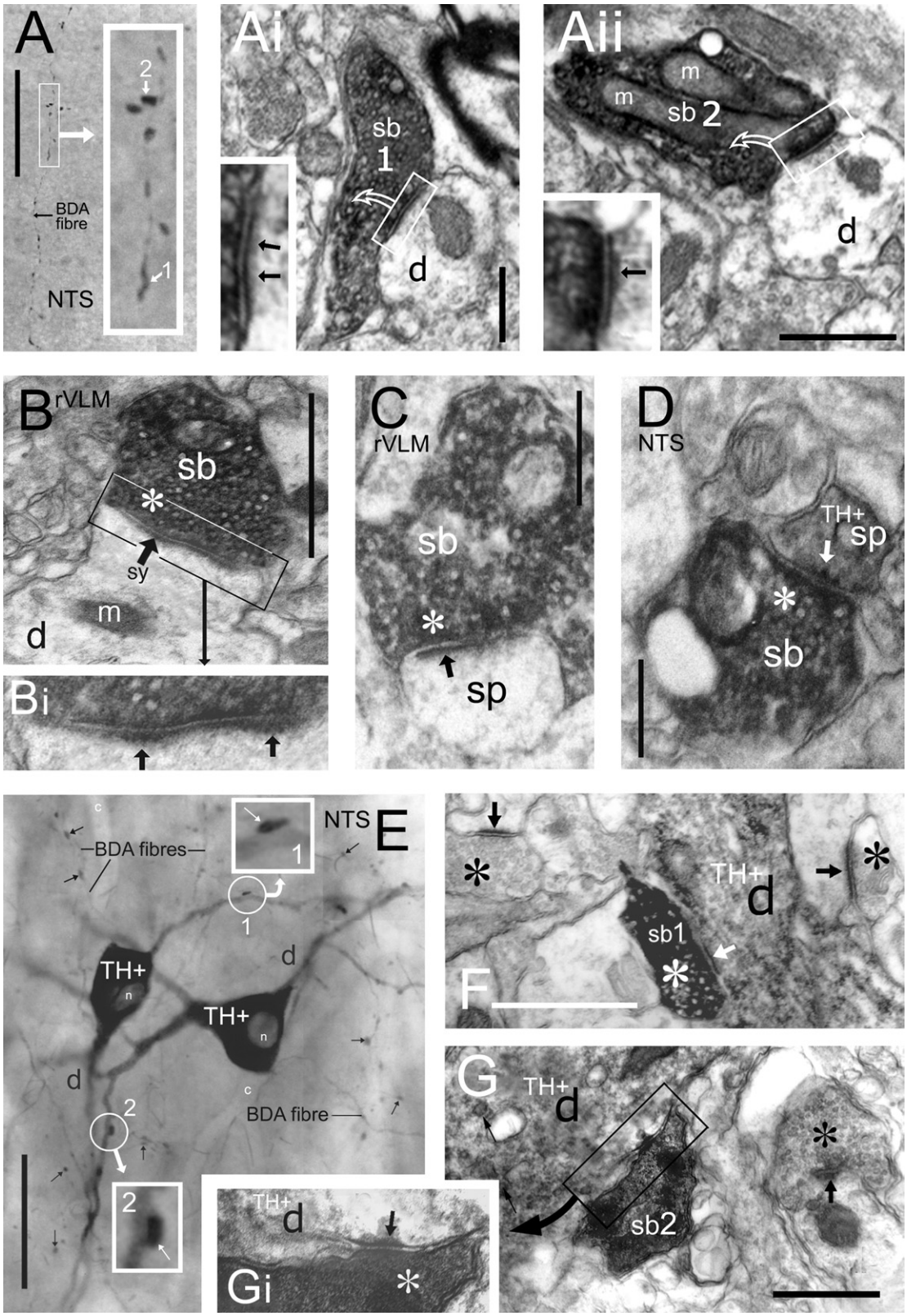

Fig. 4. (A) Light-microscope photomontage. Anterogradely labeled fine caliber BDA fiber from IL cortex in the NTS. A portion of the axonal fiber (framed area) is shown enlarged in the inset. Two axonal swellings (1, 2) are indicated. (Ai) Ultrathin section through labeled fiber swelling 1 seen in A. The labeled synaptic bouton (sb1) makes an asymmetrical synaptic junction (inset, arrows) with a small caliber distal dendritic shaft (d). Scale bar=0.5 μm. (Aii) Ultrathin section through fiber swelling 2 seen in A. The identified synaptic bouton (sb2) establishes an asymmetrical synapse (inset,

Table 1. Post-synaptic targets of BDA-labeled IL synaptic boutons in NTS and rVLM in sections immunoreacted for TH[a]

	Dendritic spines		Dendritic shafts	
	TH+	TH−	TH+	TH−
(A) NTS targets				
Animal #1	3/200 (1.5%)	55/200 (27.5%)	15/200 (7.5%)	127/200 (63.5%)
Animal #2	2/200 (1.0%)	43/200 (21.5%)	13/200 (6.5%)	142/200 (71.0%)
% Mean	1.25%	24.5%	7.0%	67.25%
(B) rVLM targets				
Animal #1	3/100 (3.0%)	14/100 (14.0%)	8/100 (8.0%)	75/100 (75.0%)
Animal #2	2/100 (2.0%)	22/100 (22.0%)	5/100 (5.0%)	71/100 (71.0%)
% Mean	2.5%	18.0%	6.5%	73.0%

[a] Two hundred BDA-labeled IL boutons with clearly identified post-synaptic targets examined in NTA and 100 such boutons examined in rVLM per animal (n=2). TH−, tyrosine hydroxylase immunonegative.

tive behaviors with underlying autonomic components (Drevets, 2000; Uylings et al., 2000). These projections are shown schematically in Fig. 5A. Interconnections between these subcortical nuclei, some of which project directly to the NTS and VLM, are considered to play a significant role in mediating the cardiovascular effects elicited by stimulation of IL cortex and adjacent areas of vmPFC (Verberne et al., 1997; Fisk and Wyss, 2000; Owens and Verberne, 2001; Krout et al., 2005).

As discussed below, TH+ neurons in the NTS and VLM are strategically involved in the regulation of cardiovascular activities and project to a variety of common supramedullary regions also innervated by descending input from IL cortex (Fig. 5A).

Functions and projections of TH+ neurons in NTS and VLM

The caudal part of the NTS, the main termination territory of afferents from IL cortex, contains catecholaminergic neurones of the A2 noradrenergic (NA) cell group (Van Giersbergen et al., 1992). Of functional significance is that a large proportion of these TH+ cells receives direct input from arterial and carotid baroreceptors, as well as arterial chemoreceptors (Owens et al., 1999; Owens and Verberne, 2000). The VLM contains two major catecholaminergic cells groups, the C1 adrenergic cell group in the rVLM and the A1 NA cell group in the dorsal cVLM (Dampney, 1994). Catecholaminergic neurons in the rVLM provide tonic and phasic regulation of baroreceptor activity (Dampney et al., 2003). Moreover, following periods of hypotension approximately two-thirds of baroresponsive neurons throughout the VLM were TH+ neurons of the A1/C1 cell groups (Dampney and Horiuchi, 2003).

Subpopulations of catecholaminergic neurons in the NTS and rVLM project to a variety of supramedullary structures that are involved in specific autonomic and neuroendocrine functions (see Fig. 5A). Estimates indicate that of TH+ neurons in the NTS, 51% project to PVN and 17% to PBN, with little overlap between the two populations (Petrov et al., 1993; Hermes et al., 2006). Of functional significance is that the TH+ NTS→PVN neurons are directly involved in cardiovascular responses (Kannan and Yamashita, 1985; Krukoff et al., 1995; Hermes et al., 2006).

arrow) with a dendritic shaft (d). Scale bar=0.5 μm. (B) An identified synaptic bouton (sb) in rVLM anterogradely labeled with BDA from IL cortex. The labeled bouton establishes an asymmetric junction (black arrow) with an unlabeled d. Synaptic vesicles (asterisk) are present in the pre-synaptic element. Mitochondrion, m. Scale bar=0.5 μm. Inset (Bi) shows the asymmetric nature of synaptic membrane specialization (black arrows), synaptic vesicles in pre-synaptic structure (asterisk) are indicated. Scale bar=0.5 μm. (C) Electron-micrograph of an identified sb in the cVLM, anterogradely labeled with BDA from IL cortex. The labeled presynaptic bouton establishes an asymmetric junction (black arrow) with an unlabeled dendritic spine head (sp). Synaptic vesicles (asterisk) are clustered near to the pre-synaptic membrane. Scale bar=0.3 μm. (D) An identified sb in the NTS, anterogradely labeled with BDA from IL cortex. The labeled bouton establishes an asymmetric junction (white arrow) with a TH+ dendritic spine head (sp). Synaptic vesicles (white asterisk) are present near the pre-synaptic membrane. Scale bar=0.2 μm. [Note: TH+ immunoreactivity is indicated by the dark diffuse SG labeling of the cytoplasm in the innervated spine head, compare the cytoplasm of the TH+ spine head with the TH− spine head seen in C.]. (E) Light-microscope photomontage. Two TH+ neurons in the caudolateral NTS with immunolabeled dendrites (d). BDA-labeled fibers from IL cortex ramify within the dendritic arbors, labeled axonal varicosities are indicated (black arrows). Two identified varicosities are closely apposed to identified TH+ processes (regions 1 and 2 circled in white). These close structural associations are shown enlarged in the respective boxes (inserts). Capillaries, c; nuclei, n. Scale bar=25 μm. (F) Correlated ultrathin section through the identified axonal varicosity shown in circled region 1 in E. [Note: Image has been rotated approximately 120° anticlockwise to the structural arrangement seen in E]. The BDA-labeled IL synaptic bouton (sb1) establishes an asymmetrical synaptic junction (white arrow) with the shaft of the TH+ dendrite (d). Synaptic vesicles are present near the presynaptic membrane specialization (asterisk). Two other asymmetrical synaptic junctions (black arrows) are present in the surrounding neuropil (black asterisks indicate clusters of synaptic vesicles). Scale bar=1.0 μm in E. (G) Correlated ultrathin section through the identified axonal varicosity shown in circled region 2 in D. The labeled synaptic bouton (sb2) is closely apposed to the shaft of the TH+ dendrite (d). An unlabeled bouton containing numerous synaptic vesicles (asterisk) makes an asymmetrical synaptic junction (arrow) with a dendritic profile. Inset Gi shows the asymmetrical nature of the synaptic membrane specialization between the identified bouton (asterisk) and the labeled TH+ dendrite (d). Scale bar=0.5 μm G.

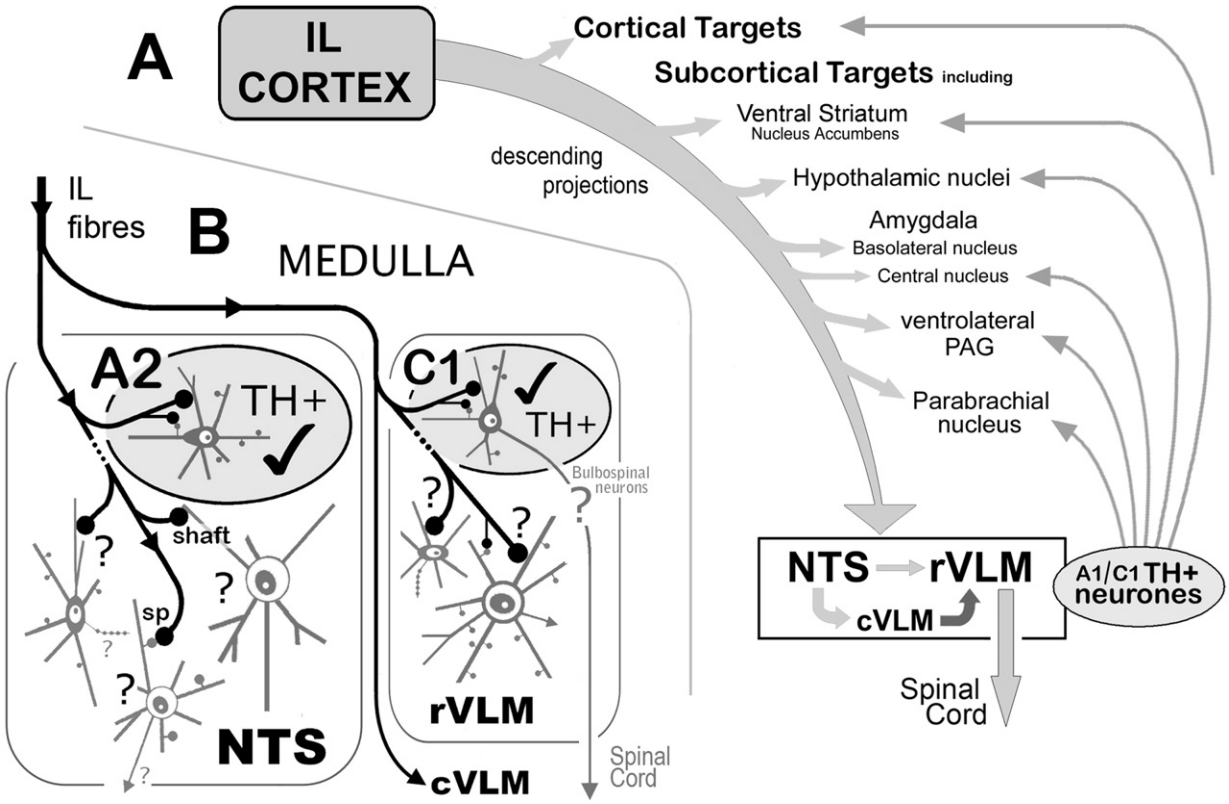

Fig. 5. Schematic diagram of the descending connectivity of the IL→NTS/VLM pathway. (A) Populations of layer 5 pyramidal cells in IL cortex (area 25) project to a range of cortical and subcortical targets that include the nucleus accumbens (VS), hypothalamic nuclei, BLA, vlPAG, PBN as well as the NTS and VLM. Previous studies indicate that populations of brainstem A1/C1 TH+ neurons have ascending projections to the aforementioned supramedullary structures. Projections from medullary regions are reported to project to the limbic forebrain including the IL (Zagon et al., 1994). (B) The major finding of this study is that pyramidal cells in IL cortex give rise to descending fibers that innervate TH+ neurons in NTS and rVLM and also contact TH+ processes in cVLM. Within NTS, identified afferents from IL cortex innervate the dendritic spines and shafts of TH+ cells, as well as the dendritic spines and small caliber distal dendritic shafts of unlabeled cells. The axonal projections of the innervated neurons are unknown (?).Whether local circuit neurons in the NTS are innervated is also unknown (?). Within rVLM, labeled afferents from IL cortex (which may be collaterals of the NTS pathways) innervate the spines and shafts of TH+ cells, as well as the spines and dendritic shafts of unlabeled cells (?). It is unknown whether IL afferents innervate local circuit neurons in the rVLM and or bulbospinal neurons.

A large proportion (78%) of TH+ neurons in the medial, intermediate, and commissural subnuclei of the NTS projects to the vlPAG, a structure involved in cardiovascular adjustments associated with fear and anxiety related behaviors (Chen et al., 1995). Moreover, Jia et al. (1997) estimate that about 80% of TH+ NTS neurons and 90% of TH+ VLM neurons project directly to CEA, which is reciprocally connected to BLA (Fig. 5A) and participates in the autonomic regulation of visceral functions involving cardiovascular, respiratory and gastrointestinal activities.

The tract-tracing study of Delfs et al. (1998) has shown that the caudal shell of the VS receives NA afferents primarily from the A2 NA cell group of the dorsomedial NTS, and to a much lesser extent from the A1 NA cell group of the cVLM and the locus coeruleus, the proportion of catecholaminergic neurons participating in these projections was not quantified. Of note is that the VS is a prominent target of projection neurons in vmPFC (Sesack et al., 1989; Ding et al., 2001; Gabbott et al., 2005).

Given the proportions that the TH+ projection neuron populations described above represent of the total number of catecholaminergic neurons in NTS and VLM, it is possible that the terminal axonal arbors of IL afferents to NTS and VLM innervate one or more of these populations.

Functional implications

Although the characteristic neurochemical, ultrastructural and functional properties of target neurons in the NTS and VLM receiving synaptic input from IL cortex need to be fully defined in future studies (Resstel and Corrêa, 2006a,b; Sevoz-Couche et al., 2006), one important question emerges from the present data: 'What are the functional implications of the comparatively modest IL input to TH+ neurons in both the NTS and rVLM?'

Immunocytochemical evidence indicates that the descending projections from IL cortex would provide 'excitatory' glutamatergic input to the dendritic shafts and spines of neurochemically diverse target neurons in both NTS and rVLM (Torrealba and Müller, 1999). Recent data in the rat indicate that neurons projecting to NTS and rVLM represent approximately 7% and 4%, respectively, of the layer 5 projection pyramidal cells in IL cortex and that

these projections mainly arise from separate neuron populations (Table 3A and Fig. 15 in Gabbott et al., 2005). Of functional significance is that the neuron populations responsible for the IL→NTS and IL→VLM projections may be embedded in different cortical networks subserving specific autonomic processes.

Descending IL input, located proximally over the dendritic arbors of identified TH+ neurons (Figs. 3; 4E; 5B), could act in concert with other cortical and subcortical inputs to provide direct 'feedback' excitatory facilitation of distinct sub-populations of TH+ NTS neurons processing different aspects of afferent cardiovascular and pulmonary information (Dampney, 1994; Dampney et al., 2003). Such synaptic circuits might significantly influence, or 'prime,' the spatiotemporal patterning of neural activity in modality specific parallel pathways through the NTS, as well as affect TH+ neurons projecting to higher brain structures, especially those in the limbic forebrain (Zagon et al., 1994). Indeed some of the supramedullary targets receiving input from TH+ NTS neurons may also receive direct convergent afferent synaptic input from IL and other areas of cortex processing complementary autonomic information (Fig. 5A). Similarly, IL innervation of rVLM TH+ neurons could, together with other inputs (Viltart and Sequeira, 1999), affect descending projections to the spinal cord from functionally specific subpopulations of TH+ bulbospinal neurons in rVLM (see Fig. 5B; Coote and Lewis, 1995).

CONCLUSION

The direct innervation of TH+ neurons in the NTS and rVLM by input from IL cortex (or other cortical areas such as the insular and motor cortices; Ba-M'Hamed et al., 1998; Hayama and Ogawa, 2001), has not been previously demonstrated ultrastructurally. The novel findings reported here identify a part of the synaptic circuitry, related to catecholaminergic A2 and C1 neurons, whereby IL 'visceromotor' cortex has a limited, yet significant, potential to influence not only the physiological integration of afferent visceral information within the NTS, but also, in parallel, affect the outflow of information from select TH+ presympathetic bulbospinal rVLM neurons. Such data provide further structural details about how the cerebral cortex is able to influence autonomic functions in rats (Neafsey, 1990; Loewy, 1991; Neafsey et al., 1993), and possibly in higher mammals and humans (Arango et al., 1988).

Acknowledgments—We thank Paul Jays (Oxford University) and Tina Wardhaugh (The Open University) for technical assistance. Grant support from the Wellcome Trust [Grant No.: 047314/96/Z/WRE/MB], Beit Memorial Fund, MRC (UK) [Grant No.: G9312936N] and the Research Committee of The Open University, Milton Keynes is acknowledged gratefully.

REFERENCES

Agarwal SK, Calarescu FR (1992) Interaction of putative neurotransmitters in rostral ventrolateral medullary cardiovascular neurons. J Auto Nerv Syst 38:159–166.

Arango V, Ruggiero DA, Callaway JL, Anwar M, Mann JJ, Reis DJ (1988) Catecholaminergic neurons in the ventrolateral medulla and nucleus of the solitary tract in the human. J Comp Neurol 273:224–240.

Bacon SJ, Headlam AJN, Gabbott PLA, Smith AD (1996) Amygdala input to medial prefrontal cortex (mPFC) in the rat: a light and electron microscope study. Brain Res 720:211–219.

Bacon SJ, Gabbott PLA (1997) Infralimbic cortex (area 25) monosynaptically innervates subcortical autonomic midbrain and brainstem regions in the rat. J Autonom Nerv Syst 65(2/3):97.

Ba-M'Hamed S, Viltart O, Poulain P, Sequeira H (1998) Distribution of cortical fibers and Fos immunoreactive neurons in ventrolateral medulla and in nucleus tractus solitarius following the motor cortex stimulation in the rat. Brain Res 813:411–415.

Bolam JP (Ed) (1992) Experimental neuroanatomy: a practical approach. Oxford: IRL Press.

Cechetto DF, Saper C (1990) Role of the cerebral cortex in autonomic functions. In: Central regulation of autonomic functions (Loewy D, Spyer KM, eds), pp 208–223. New York: Oxford University Press.

Chen L-W, Rao Z-R, Shi J-W (1995) Catecholaminergic neurons in the nucleus tractus solitarii which send their axons to midbrain periaqueductal gray express Fos protein after noxious stimulation of the stomach: a triple labelling study in the rat. Neurosci Lett 189:179–181.

Cobos A, Lima D, Almeida A, Tavares I (2003) Brain afferents to the lateral caudal ventrolateral medulla: A retrograde and anterograde tracing study in the rat. Neuroscience 120:485–498.

Coote JH, Lewis DI (1995) Bulbospinal catecholamine neurones and sympathetic pattern generation. J Physiol Pharmacol 46:259–271.

Dampney RA, Horiuchi J (2003) Functional organisation of central cardiovascular pathways: studies using c-fos gene expression. Prog Neurobiol 71:359–384.

Dampney RA, Polson JW, Potts PD, Hirooka Y, Horiuchi J (2003) Functional organisation of brain pathways subserving the baroreceptor reflex: studies in conscious animals using immediate early gene expression. Cell Mol Neurobiol 23:597–616.

Dampney RAL (1994) Functional organisation of central pathways regulating the cardiovascular system. Physiol Rev 74:323–364.

Delfs JM, Zhu Y, Druhan JP, Aston-Jones GS (1998) Origin of noradrenergic afferents to the shell subregion of the nucleus accumbens: anterograde and retrograde tract-tracing studies in the rat. Brain Res 806:127–140.

Ding CD, Gabbott PLA, Totterdell S (2001) Differences in the laminar origin of projections from the medial prefrontal cortex to the nucleus accumbens shell and core regions in the rat. Brain Res 917:81–89.

Drevets WC (2000) Functional anatomical abnormalities in limbic and prefrontal cortical structures in major depression. In: Progress in brain research, Vol. 126 (Uylings HBM, Van Eden CG, DeBruin JPC, Feenstra MGP, Pennartz CMA, eds), pp 413–431. Amsterdam: Elsevier.

Fisk GD, Wyss JM (2000) Descending projections of infralimbic cortex that mediates stimulation-evoked changes in arterial pressure. Brain Res 859:83–95.

Gabbott P, Headlam A, Busby S (2002) Morphological evidence that CA1 hippocampal afferents monosynaptically innervate PV-containing neurons and NADPH-diaphorase reactive cells in the medial prefrontal cortex (areas 25/32) of the rat. Brain Res 946:314–322.

Gabbott PLA, Warner TA, Jays PRL, Salway P, Busby SJ (2005) Prefrontal cortex in the rat: Projections to subcortical autonomic, limbic and motor centres. J Comp Neurol 377:465–499.

Gray EG (1959) Axo-somatic and axo-dendritic synapses of the cerebral cortex: an electron microscope study. J Anat 93:420–433.

Groenewegen HJ, Uylings HB (2000) The prefrontal cortex and the integration of sensory, limbic and autonomic information. Prog Brain Res 126:3–28.

Halliday GM, McLachlan EM (1991) Four groups of tyrosine hydroxylase-immunoreactive neurons in the ventrolateral medulla of rats, guinea-pigs and cats identified on the basis of chemistry, topography and morphology. Neuroscience 43:551–568.

Hardy SG, Mack SM (1990) Brainstem mediation of prefrontal stimulus produced hypotension. Exp Brain Res 79:393–399.

Hayama T, Ogawa H (2001) Two loci of the insular cortex project to the taste zone of the nucleus of the solitary tract in rats. Neurosci Lett 303:49–52.

Heidbreder CA, Groenewegen HJ (2003) The medial prefrontal cortex in the rat: evidence for a dorso-ventral distinction based upon functional and anatomical characteristics. Neurosci Biobehav Rev 27:555–579.

Hermes SM, Mitchell JL, Aicher SA (2006) Most neurons in the nucleus tractus solitarii do not send collateral projections to multiple autonomic targets in the rat brain. Exp Neurol 198:539–551.

Howard V, Reed C (2005) Unbiased stereology: three-dimensional measurement in microscopy. Microscopy handbooks 41. Guildford: Bios Scientific Publishers/Royal Microscopical Society.

Hurley KM, Herbert H, Moga MM, Saper CB (1991) Efferent projections of the infralimbic cortex of the rat. J Comp Neurol 308: 249–276.

Hussain Z, Johnson L, Totterdell S (1996) A light and electron microscopic study of NADPH-diaphorase-, calretinin- and parvalbumin-containing neurons in the rat nucleus accumbens. J Chem Neuroanat 10:19–39.

Jia H-G, Rao Z-R, Shi J-W (1997) Evidence of γ-aminobutyric acidergic control over the catecholaminergic projection from the medulla oblongata to the central nucleus of the amygdala. J Comp Neurol 381:262–281.

Kannan M, Yamashita H (1985) Connections of neurons in the region of the nucleus tractus solitarius with the hypothalamic paraventricular nucleus: their possible involvement in neural control of the cardiovascular system in rats. Brain Res 329:205–212.

Krout KE, Mettenleiter TC, Karpitskiy V, Van Nguyen X, Loewy AD (2005) CNS neurons links to both mood-related cortex and sympathetic nervous system. Brain Res 1050:199–202.

Krukoff TL, MacTavish D, Harris KH, Jhamandas JH (1995) Changes in blood volume and pressure induce *c-fos* expression in brainstem neurons that project to the paraventricular nucleus of the hypothalamus. Mol Brain Res 34:99–108.

Kubo T, Goshima Y, Hata H, Misu Y (1990) Evidence that endogenous catecholamines are involved in alpha-2-adrenoceptor mediated modulation of the aortic baroceptor reflex in the nucleus tractus solitarii of the rat. Brain Res 526:313–317.

Loewy AD (1991) Forebrain nuclei involved in autonomic control. Prog Brain Res 87:253–268.

Millenbruck EW, Wallinga MH (1946) A newly developed anaesthetic for horses. J Am Vet Med Assoc 108:148–151.

Murphy AZ Ennis M, Shipley MT, Behbehani MM (1994) Directionally specific changes in arterial pressure induce differential patterns of Fos expression in discrete areas of the rat brainstem: A double-labeling study for Fos and catecholamines. J Comp Neurol 349:36–50.

Neafsey EJ, Hurley-Guis KM, Arvantis D (1986) The topographical organisation of neurons in the medial frontal, insular and olfactory cortex projecting to the solitary nucleus, olfactory bulb, periaqueductal grey and superior colliculus. Brain Res 377:261–270.

Neafsey EJ (1990) Prefrontal cortical control of the autonomic nervous system: anatomical and physiological observations. Prog Brain Res 85:147–166.

Neafsey EJ, Terreberry RR, Hurley KM, Ruit KG, Frysztak RJ (1993). Anterior cingulate cortex in rodents: connections, visceral control functions, and implications for emotion. In: Neurobiology of cingulate cortex and limbic thalamus: a comprehensive handbook (Vogt BA, Gabriel M, eds), pp 206–223. Boston: Birkhaüser.

Owens NC, Verberne AJM (1996) An electrophysiological study of the medial prefrontal cortex projection to the nucleus of the solitary tract in rat. Exp Brain Res 110:55–61.

Owens NC, Sartor DM, AJM Verberne (1999) Medial prefrontal cortex depressor response: role of the solitary tract nucleus in the rat. Neuroscience 89:1331–1346.

Owens NC, Verberne AJ (2000) Medial prefrontal depressor response: involvement of the rostral and caudal ventrolateral medulla in the rat. J Auton Nerv Syst 78:86–93.

Owens NC, Verberne AJM (2001) Regional haemodynamic responses to activation of the medial prefrontal cortex depressor region. Brain Res 919:221–231.

Paxinos G, Carrive P, Wang H, Wang P-Y (1999) Chemoarchitectonic atlas of the rat brainstem. London: Academic Press.

Petrov T, Krukoff T, Jhamandas JH (1993) Branching projections of catecholaminergic brainstem neurons to the paraventricular hypothalamic nucleus and the central nucleus of the amygdala in the rat. Brain Res 609:81–92.

Resstel LBM, Corrêa FMA (2006a) Medial prefrontal cortex NMDA receptors and nitric oxide modulate the parasympathetic component of the baroreflex. Eur J Neurosci 23:481–488.

Resstel LBM, Corrêa FMA (2006b) Involvement of the medial prefrontal cortex in central cardiovascular modulation in the rat. Auton Neurosci 126/127:130–138.

Ruit KG, Neafsey EJ (1990) Hippocampal input to a 'visceral motor' corticobulbar pathway: an anatomical and electrophysiological study in the rat. Exp Brain Res 82:505–616.

Sesack SR, Deutch AY, Roth RH, Bunney BS (1989) Topographical organisation of the efferent projections of the medial prefrontal cortex in the rat: an anterograde tract-tracing study with *Phaseolus vulgaris leucoagglutinin*. J Comp Neurol 290:213–242.

Sevoz-Couche C, Comet MA, Bernard JF, Hamon M, Lagozzi R (2006) Cardiac baroreflex facilitation evoked by hypothalamus and prefrontal cortex stimulation: role of nucleus tractus solitarius (NTS) 5-HT2A receptors. Am J Physiol Integr Comp Physiol 291:R1007–R1015.

Spyer KM (1994) Annual review prize lecture: Central nervous mechanisms contributing to cardiovascular control. J Physiol 474:1–19.

Swanson LW (1998) Brain maps: structure of the rat brain, 2nd ed. Amsterdam: Elsevier.

Takagishi M, Chiba T (1991) Efferent projections of the infralimbic (area 25) region of the medial prefrontal cortex in the rat: an anterograde tracer PHA-L study. Brain Res 566:26–39.

Tavares RF, Antunes-Rodrigues J, de Aguiar Correa FM (2004) Pressor effects of electrical stimulation of medial prefrontal cortex in unanaesthetised rats. J Neurosci Res 77:613–620.

Terreberry R, Neafsey EJ (1987) The rat medial frontal cortex projects directly to autonomic regions of the brainstem. Brain Res Bull 19:639–649.

Torrealba F, Müller C (1999) Ultrastructure of glutamate and GABA immunoreactive terminals of the rat nucleus tractus solitarius, with a note on infralimbic cortex afferents. Brain Res 820: 20–30.

Uylings HBM, van Eden GG, de Bruin JPC, Feenstra MGP, Pennartz CMA, eds (2000) Cognition, emotion and autonomic responses: the integrative role of the prefrontal cortex and limbic structures. Amsterdam: Elsevier.

Uylings HB, Groenewegen HJ, Kolb B (2003) Do rats have a prefrontal cortex? Behav Brain Res 146:3–17.

Van Eden CG, Buijs RM (2000) Functional neuroanatomy of the prefrontal cortex: autonomic interactions. In: Progress in brain research, Vol. 126 (Uylings HBM, Van Eden CG, DeBruin JPC, Feenstra MGP Pennartz CMA, eds), pp 49–62. Amsterdam: Elsevier.

Van Giersbergen PL, Palkovits M, De Jong W (1992) Involvement of neurotransmitters in the nucleus tractus solitarii in cardiovascular regulation. Physiol Rev 72:789–824.

Verberne AJ, Lam W, Owens NC, Sartor D (1997) Supramedullary modulation of sympathetic vasomotor function. Clin Exp Pharmacol Physiol 24:748–754.

Verberne AJ, Owens NC (1998) Cortical modulation of the cardiovascular system. Prog Neurobiol 54:149–168.
Vertes RP (2004) Differential projections of the infralimbic and prelimbic cortex in the rat. Synapse 51:32–58.
Viltart O, Sequeira H (1999) Induction of c-Fos-like protein in bulbar catecholaminergic neurones by electrical stimulation of the sensorimotor cortex in the rat. Neurosci Lett 260:65–88.
Yasui Y, Itoh K, Kaneko T, Shigemoto R, Mizuno N (1991) Topographical projections from the cerebral cortex to the nucleus of the solitary tract in the cat. Exp Brain Res 85:75–84.
Zagon A, Totterdell S, Jones RS (1994) Direct projections from the ventrolateral medulla oblongata to the limbic forebrain: anterograde and retrograde tract-tracing studies in the rat. J Comp Neurol 340:445–468.

(Accepted 17 September 2006)
(Available online 13 November 2006)